

Image processing for maturity classification of tomato using otsu and manhattan distance methods

Anindita Septiari ^{a,1,*}, Hamdani Hamdani ^{a,2}, Muhammad Sofian Sauri ^{a,3}, Joan Angelina Widians ^{a,4}

^a Department of Informatics, Faculty of Engineering, Mulawarman University, Samarinda, Indonesia

¹ anindita@unmul.ac.id; ² hamdani@unmul.ac.id; ³ sofianoutsiders@gmail.com; ⁴ angelinajo@fkti.unmul.ac.id

* Corresponding Author

Received 17 October 2021; accepted 20 February 2022; published 23 February 2022

ABSTRACT

Currently, image processing-based systems have been widely applied in various fields, one of which is agriculture. The system can be used to classify fruit maturity. Tomato is one of the agricultural products consumed by the community. Therefore, the requirement for ripe tomatoes increases. In this work, the classification method based on image processing for grading the maturity level of tomato was developed to distinguish tomato into three classes: unripe, half-ripe, and ripe. Classification is carried out based on the skin color of the tomato. The method required five main processes; initially, the detection of the region of interest (ROI) applied using the Otsu method followed by the conversion of RGB to HSV color space. Afterward, segmentation with Otsu thresholding on the S channel of the HSV color space was implemented. Subsequently, the extraction of the mean, median, max, and min features on each channel from the YIQ color space; therefore, a total number of 12 features was produced. Finally, the K-nearest neighbor (KNN) method using Manhattan distance is applied with the values of $k = 1, 3, 5, 7,$ and 9 . The dataset used consists of 90 images of tomatoes (30 raws, 30 half-ripes, and 30 ripes), where the dataset is divided into two types, including 54 images as training data and 36 images as testing data. The evaluation results were able to achieve the highest accuracy value of 0.9722.



KEYWORDS

Pre-processing
Segmentation
Otsu
Features extraction
Classification



This is an open-access article under the [CC-BY-SA](https://creativecommons.org/licenses/by-sa/4.0/) license

1. Introduction

Currently, image processing-based computer systems have been widely applied and are still being developed in various fields. In the plantation sector, image processing has been used for several purposes, namely detecting plant diseases [1] [2] [3] and determining fruit quality based on the level of maturity. Determination of the quality requires a detection process or maturity classification. Research related to the classification of fruit maturity has been applied to several kinds of fruit such as palm [4], [5] oranges [6], apples [7], pomegranates [8], passion fruit [9], and tomatoes [10].

Classification of tomato fruit maturity needs to be investigated because tomatoes are one of the most needed plantation products. Tomatoes can be consumed directly or processed into processed foods so that they last longer. Tomatoes are widely consumed because they contain lots of fiber, useful nutrients such as antioxidants, vitamins C and A for eye health, and also daily diet and tastes good. Therefore, the need for tomatoes of good quality continues to increase. The level of maturity influences the quality of tomatoes to affect the nutritional content of the fruit. Accordingly, this study proposes a method for detecting tomato ripeness that requires three main processes: segmentation, feature extraction, and classification.

The segmentation process is a task to distinguish the tomato area and the background. This process is needed due to only the tomato area is applied to the feature extraction process. The studies related to segmentation have been implemented on various fruit, including apple [11], [12], mango [13], strawberry [14], palm [15], and tomato [16]. The method is commonly used for the segmentation process on fruit objects such as threshold-based [17], [6], and edge detection using several operators including Sobel [18], Prewitt [19], and Canny [15].

Meanwhile, the feature extraction process is a process to generate values that are used to distinguish the maturity level of tomatoes. This value will be used as input in the classification process. In previous studies, the most widely used feature related to fruit maturity is the color feature [5], [6]. Furthermore, the classification process is needed to determine fruit's class or level of maturity based on the test image entered in the system. One of the most widely applied classification methods for fruit ripening is K-Nearest Neighbors (KNN). This method has been implemented for the classification of several kinds of fruit, including avocado [20], orange [6], [21], and tomato [22].

The contribution of this study is to apply the Otsu and KNN methods with Manhattan distance using color features to classify the tomato maturity based on fruit skin color. Image processing technique was carried out to develop this method. Classification distinguishes tomatoes into three classes: unripe, half-ripe, or ripe. The input data was an image of a tomato acquired using a smartphone. Smartphones were chosen due to their ease of use and accessibility.

2. Method

The method applied in this study received input data in a tomato image (original image). The image of tomatoes used consists of three types distinguished based on the level of maturity: raw, half-ripe, and ripe, which have different skin colors. This method consists of five main processes, namely: (1) ROI detection, (2) pre-processing, (3) segmentation, (4) feature extraction, and (5) classification, where each main process consists of several steps. The main process steps of the applied method, along with several examples of the original image, are shown in Fig. 1.

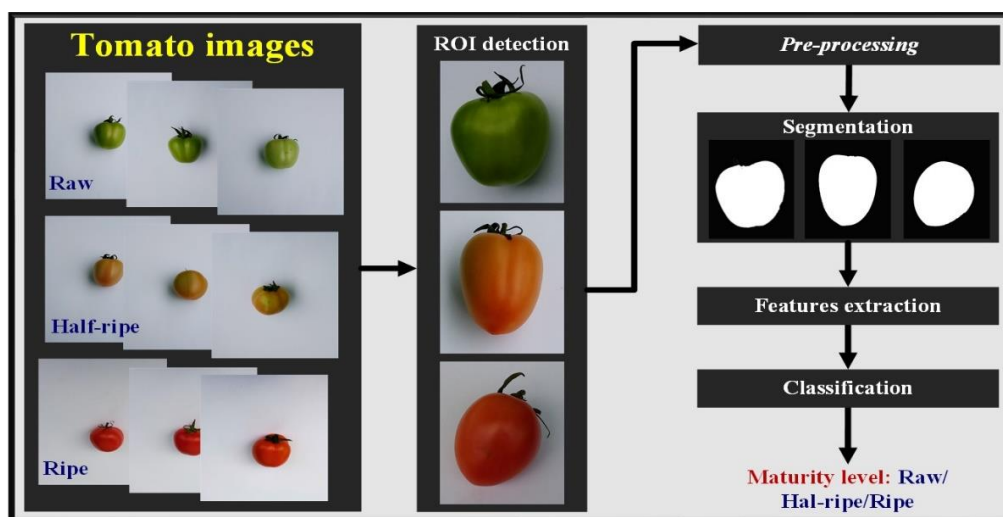


Fig. 1. The main process on tomato maturity classification.

2.1. Tomato Dataset

The dataset used in this study consisted of 90 images of tomatoes. It includes 30 raw images, 30 half-ripe images, and 30 ripe images. Those images were acquired using a smartphone with a 16-megapixel camera. The distance between the camera and the object is ± 20 cm which is saved in JPEG format with 3456×4608 pixels. The tomato object was acquired using a white background with bright and even lighting. An example of the tomato image acquisition results can be seen in Fig. 1.

2.2. Deteksi ROI

ROI detection is a process that aims to form sub-images (ROI images) that focus more on loading the tomato area and speed up the following process. This process begins by resizing the original image (resize) of 3456×4608 pixels to 1728×2304 pixels (0.5 smaller than the original size). Furthermore, the Otsu thresholding method is applied to detect the tomato area, followed by determining the area boundary for the formation of ROI images. Fig. 2 shows an image of the results of each step in the ROI detection process.

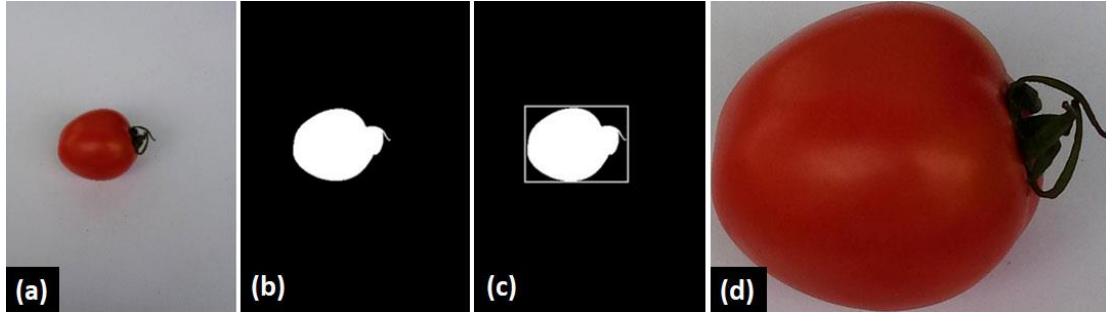


Fig. 2. The examples of images resulting from each step in the ROI detection process: (a) resizing, (b) Otsu thresholding, (c) determining ROI image boundaries, and (d) ROI images

The Otsu method aims to obtain the optimal threshold value by first converting the ROI image into a grayscale image. The steps of the Otsu method algorithm are as follows [23]:

1. Set a histogram from the grayscale ROI image with intensity values from i to L , where the value of i starts from the lowest to the highest intensity, i.e., 0 to 255. The probability that each pixel has an intensity of i is stated in equation (1)

$$P_i = \frac{n_i}{N}, P_i \geq 0, \sum_{i=1}^L P_i = 1. \quad (1)$$

2. Calculate the cumulative value of intensity probability (ω_k) for $L = 0, 1, 2, 3, \dots, L-1$ defined by equation (2)

$$\omega_k = \sum_{i=0}^k P_i. \quad (2)$$

3. Calculate the cumulative mean (μ_k) for $L = 0, 1, 2, 3, \dots, L-1$ with equation (3)

$$\mu_k = \sum_{i=0}^k i \cdot P_i. \quad (3)$$

4. Calculate the average of all intensity values (μ_T) with equation (4)

$$\mu_T = \sum_{i=1}^L i \cdot P_i. \quad (4)$$

5. Calculate the value of variance between classes ($\sigma_B^2(k)$) using equation (5)

$$\sigma_B^2(k) = \frac{[\mu_T \omega_k - \mu_k]^2}{\omega_k [1 - \omega_k]}. \quad (5)$$

6. The optimal threshold value is obtained by equation (6)

$$\sigma_B^2(k) = \max_{1 \leq k \leq L} \sigma_B^2(k). \quad (6)$$

7. Sort and select the highest value, where the k value with the highest variance is set as the threshold value.

2.3. Pre-processing

This process aims to improve image quality to make the tomato area easier to distinguish from the background area. The following process (segmentation) is more optimal to determine the tomato and background areas by adjusting the color space. In this study, the RGB to HSV color space was converted because this color space has been applied to segment fruit objects with promising results. The RGB to HSV color space conversion is defined in equations (7) to (10) [5]:

$$H = \begin{cases} \theta, & B \leq G \\ 360 - \theta, & B > G \end{cases} \quad (7)$$

$$\theta = \cos^{-1} \left\{ \frac{\frac{1}{2} [(R - G) + (R - B)]}{[x(R - G)^2 + (R - B)(G - B)]^{1/2}} \right\} \quad (8)$$

$$S = \begin{cases} 0, & \max(R, G, B) = 0 \\ 1 - \frac{\min(R, G, B)}{\max(R, G, B)}, & \text{otherwise} \end{cases} \quad (9)$$

$$V = \max(R, G, B) \quad (10)$$

2.4. Segmentation

Segmentation aims to distinguish the tomato area and the background. This process was needed; hence the subsequent process, namely feature extraction, only applied to the tomato area. In this study, segmentation was carried out using the Otsu method, with the best results being applied on the S channel compared to H and V channels. The comparison of segmentation results on channels H, S, and V is shown in Fig. 3.

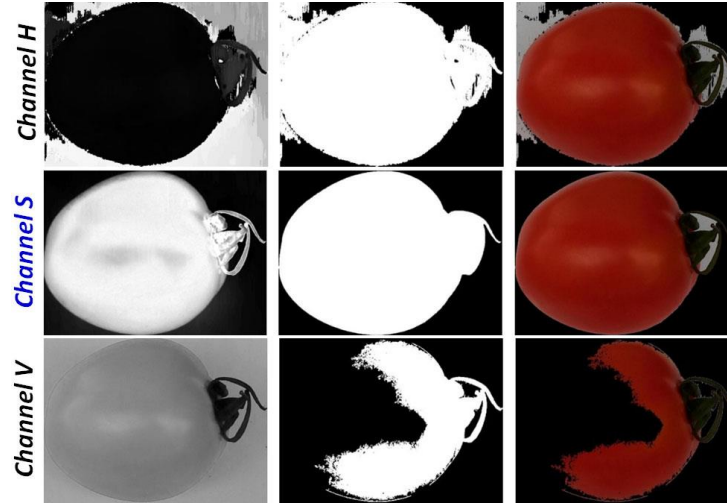


Fig. 3. The comparison of HSV color space segmentation results on H, S, and V . channels.

2.5. Features Extraction

In this study, the features were extracted based on the color of the fruit skin. Features are extracted on the YIQ color space. The YIQ color space was chosen because it can obtain optimal accuracy results. The conversion of the RGB color space to YIQ is defined in equation (11) [5].

$$\begin{bmatrix} Y \\ I \\ Q \end{bmatrix} = \begin{bmatrix} 0.299 & 0.587 & 0.114 \\ 0.596 & -0.274 & -0.322 \\ 0.211 & -0.523 & 0.312 \end{bmatrix} \begin{bmatrix} R \\ G \\ B \end{bmatrix} \quad (11)$$

The features used to consist of mean, median, minimum (min), and maximum (max). These features are extracted on each channel from the YIQ color space. The total number of features generated from one image is 12 features, namely: Ymean, Imean, Qmean, Ymedian, Imedian, Qmedian, Ymax, Imax, Qmax, Ymin, Imin, and Qmin. The value of these features is obtained from equations (12) to (16) as follows:

1. Mean (μ) is the distribution of grayscale image intensity values. The value of an image with a number of n pixels, frequency (f), gray intensity (f_n), the probability of occurrence of pixel intensity values in the histogram ($p(f_n)$) are defined in equations (12) and (13).

$$\mu = \sum_n f_n p(f_n) \quad (12)$$

$$p(f_n) = \frac{f}{\sum f} \quad (13)$$

2. Median (m) indicates the value of the center intensity of an image calculated by equation (14), where x is the lower limit, f_i is the frequency of pixels in the median class, f_j is the cumulative frequency of pixels below the median class, and p is the interval.

$$m = x + \left(\frac{\frac{f}{2} - f_{ii}}{f_i} \right) p. \quad (14)$$

3. Maximal (max) indicates the highest intensity (i) value in an image defined in equation (15)

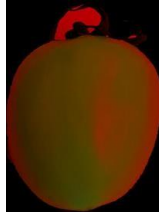
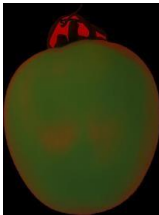
$$max = max(i). \tag{15}$$

4. Minimum (min) indicates the lowest intensity value in an image defined in equation (16)

$$min = min(i). \tag{16}$$

Examples of feature extraction result from three maturity level tomatoes: raw, half-ripe, and ripe are shown in Table 1.

Table 1. The resulting examples of feature extraction on three maturity levels of tomatoes

No.	ROI image (RGB)	YIQ image	Feature Extraction Results	
1			Class = Raw $Y_{mean} = 0.1363$ $Y_{max} = 0.4432$ $I_{mean} = 0.0247$ $I_{max} = 0.0876$ $Q_{mean} = -0.0479$ $Q_{max} = 0.0148$ $Y_{median} = 0.1802$ $Y_{min} = 0$ $I_{median} = 0.0344$ $I_{min} = -0.0230$ $Q_{median} = -0.0720$ $Q_{min} = -0.1175$	
2			Class = Half-ripe $Y_{mean} = 0.2491$ $Y_{max} = 0.668$ $I_{mean} = 0.1324$ $I_{max} = 0.2940$ $Q_{mean} = -0.0224$ $Q_{max} = 0.0430$ $Y_{median} = 0.2914$ $Y_{min} = 0$ $I_{median} = 0.2054$ $I_{min} = -0.0347$ $Q_{median} = -0.0246$ $Q_{min} = -0.1149$	
3			Class = Ripe $Y_{mean} = 0.1597$ $Y_{max} = 0.6026$ $I_{mean} = 0.1765$ $I_{max} = 0.3196$ $Q_{mean} = 0.0497$ $Q_{max} = 0.1004$ $Y_{median} = 0.2078$ $Y_{min} = 0$ $I_{median} = 0.2675$ $I_{min} = -0.0002$ $Q_{median} = 0.0749$ $Q_{min} = -0.0424$	

2.6. Classification

The KNN approach was used to classify the maturity of tomatoes. KNN is a data classification method based on the value of k , which is the nearest neighbor distance between the training and test data values. This method is employed because it is a straightforward process used to solve classification issues for a variety of objects. The KNN method has the following steps [21]:

1. Determine the value of k , which is the number of nearest neighbors.
2. Calculate the value of each testing data's square of the Euclidean distance from the training data.
3. Sort the data based on the lowest Euclidean distance to the highest.
4. The prediction class is obtained based on the class of the most majority nearest neighbor.

In this study, KNN was applied using three distance calculations, namely Euclidean, Minkowski, and Manhattan. The value of k used consists of several alternatives, including $k = 1, 3, 5, 7,$ and 9 [22], [23]. This is done to obtain optimal classification results. The calculation of Euclidean, Minkowski, and Manhattan distances is defined in equations (17) to (19) [21].

1. Euclidean

$$d = \sqrt{\sum_{i=1}^n (P_i - Q_i)^2} \tag{17}$$

where d defines the distance value, and n indicates the amount of data. Meanwhile, P_i and Q_i are i data from testing data and i data from training data.

2. Minkowski

$$d(x, y) = \left(\sum_{i=1}^n |x_i - y_i|^p \right)^{1/p} \tag{18}$$

where d defines the distance between x (the value of training data) and y (value of testing data). Meanwhile, i , n , and p indicate i -th data, the amount of data, and the power. Furthermore, x_i and y_i are the value on the i -th training data and the value on the i -th testing data.

3. Manhattan

$$d(x, y) = \sum_{i=1}^n |x_i - y_i| \tag{19}$$

where d defines the distance between x (the value of training data) and y (value of testing data). Meanwhile, i and n , indicate i -th data and the amount of data. Furthermore, x_i and y_i are the value on the i -th training data and the value on the i -th testing data.

3. Results and Discussion

The evaluation was carried out using a multi-class confusion matrix on the tomato maturity classification method based on applied skin color. Classification is divided into three classes consisting of raw (T1), half-ripe (T2), and ripe (T3). The confusion matrix for the three types of classes is shown in Table 2.

Table 2. Confusion matrix with three kinds of classes

		Prediction Class		
		T1	T2	T3
Actual class	T1	X ₁₁	X ₁₂	X ₁₃
	T2	X ₂₁	X ₂₂	X ₂₃
	T3	X ₃₁	X ₃₂	X ₃₃

Meanwhile, three parameters, namely precision, recall, and accuracy, were calculated to determine the performance of the method. The three parameters are calculated using equations (20) to (22), where n is the number of images as test data [5].

1. Precision

$$Precision = \frac{X_{ii}}{\sum_{k=1}^n X_{ki}} \tag{20}$$

2. Recall

$$Recall = \frac{N_{ii}}{\sum_{k=1}^n N_{ik}} \tag{21}$$

3. Accuracy

$$Accuracy = \frac{\sum_{i=1}^n X_{ii}}{\sum_{i=1}^n \sum_{j=1}^n X_{ij}} \tag{22}$$

The values of precision, recall, and accuracy produced are between 0 to 1. The method's performance is classified as good if the values generated by the three parameters are close to 1.

The applied method was tested using a dataset consisting of 90 images of tomatoes (30 unripe, 30 half-ripe, and 30 ripe). The dataset is divided into two parts, namely 60% (54 images) as training data and 40% (36 images) as test data. The applied method's evaluation results are measured based on three parameters, namely precision, recall, and accuracy. Table 3 shows the overall results of the KNN technique evaluation using three different distance calculation algorithms and k values. Euclidean, Minkowski, and Manhattan distance calculations were utilized, with k values of 1, 3, 5, 7, and 9 used.

Table 3 shows the application of distance calculations using Euclidean and Minkowski obtained the same results. Maximum results for precision, recall, and accuracy was obtained with a value of $k = 9$, which reached 0.9714, 0.9714, and 0.9444, respectively. Meanwhile, Manhattan produced the highest precision, recall, and accuracy values of 1.0, 0.9722, and 0.9722, respectively, which were generated using different k values.

Table 3. Evaluation result of tomato classification method based on skin color

No.	Distance algorithm	K value	Evaluation parameters		
			Precision	Recall	Akurasi
1	<i>Euclidean</i>	1	0.9429	0.9706	0.9167
2		3	0.9429	0.9706	0.9167
3		5	0.9429	0.9706	0.9167
4		7	0.9429	0.9706	0.9167
5		9	0.9714	0.9714	0.9444
6	<i>Minkowski</i>	1	0.9429	0.9706	0.9167
7		3	0.9429	0.9706	0.9167
8		5	0.9429	0.9706	0.9167
9		7	0.9429	0.9706	0.9167
10	<i>Manhattan</i>	9	0.9714	0.9714	0.9444
11		1	1.0	0.9722	0.9722
12		3	1.0	0.9722	0.9722
13		5	1.0	0.9722	0.9722
14		7	1.0	0.9722	0.9722
15	9	1.0	0.9722	0.9722	

The results of the classification of tomato maturity based on color features using the Manhattan distance calculation are shown in Table 4. Table 4 shows the confusion matrix, consisting of three classes: raw, half-ripe, and ripe. All raw and half-ripe tomato grade images were correctly predicted according to their actual grade. Meanwhile, an image of a ripe tomato was misclassified as a half-ripe tomato.

Table 4. Confusion matrix with Manhattan distance calculation for k values = 1, 3, 5, 7, and 9

		Kelas Prediksi		
		Raw	Half-ripe	Ripe
Actual class	Raw	12 (0.3333)	0 (0)	0 (0)
	Half-ripe	0 (0)	12 (0.3333)	1 (0.0278)
	Ripe	0 (0)	0 (0)	11 (0.3057)

This error is possible because visually, the color of ripe grade tomatoes is closer to half-ripe grade. Meanwhile, errors in applying distance calculations using Euclidean and Minkowski also occur in ripe tomatoes, which are classified as half-ripe or vice versa. Based on Table 1 regarding the results of feature extraction and Table 4, although the area of the tomato petals/crown is included as a feature extraction area, the classification results show that the method applied achieves an accuracy value of 0.9722. This value indicates that there is one misclassified image. This is because the tomato area is much wider than the crown.

4. Conclusion

In this study, the classification method of tomato maturity consisted of five main processes: ROI detection, pre-processing, segmentation, feature extraction, and classification. The Otsu method is applied in the ROI detection and segmentation process, while the RGB to HSV color space is converted in the pre-processing. Meanwhile, the color feature is used for each channel of the YIQ color space. The extracted features consist of mean, median, minimum (min), and maximum (max) so that the total features produced are 12. Furthermore, in the classification process, the KNN method is applied using Manhattan distance calculations with k = 1, 3, 5, 7, and 9. The method applied was tested using a dataset consisting of 90 tomato images and managed to achieve an accuracy value of 0.9722. Based on the test results, the features and methods applied are suitable for the dataset used in this study.

Acknowledgment

The author appreciates the support and research funds provided by the Faculty of Engineering, Mulawarman University in 2021.

Declarations

Author contribution. All authors contributed equally to the main contributor to this paper. All authors read and approved the final paper.

Funding statement. This research was funded by the Faculty of Engineering, Mulawarman University in 2021.

Conflict of interest. The authors declare no conflict of interest.

Additional information. No additional information is available for this paper.

References

- [1] S. Zhang, S. Zhang, C. Zhang, X. Wang, and Y. Shi, "Cucumber leaf disease identification with global pooling dilated convolutional neural network," *Comput Electron Agric*, vol. 162, pp. 422–430, Jul. 2019, doi: [10.1016/J.COMPAG.2019.03.012](https://doi.org/10.1016/J.COMPAG.2019.03.012).
- [2] X. E. Pantazi, D. Moshou, and A. A. Tamouridou, "Automated leaf disease detection in different crop species through image features analysis and One Class Classifiers," *Comput Electron Agric*, vol. 156, pp. 96–104, Jan. 2019, doi: [10.1016/J.COMPAG.2018.11.005](https://doi.org/10.1016/J.COMPAG.2018.11.005).
- [3] G. Geetharamani and A. P. J., "Identification of plant leaf diseases using a nine-layer deep convolutional neural network," *Computers & Electrical Engineering*, vol. 76, pp. 323–338, Jun. 2019, doi: [10.1016/J.COMPELECENG.2019.04.011](https://doi.org/10.1016/J.COMPELECENG.2019.04.011).
- [4] A. Septiarini, H. R. Hatta, H. Hamdani, A. Oktavia, A. A. Kasim, and S. Suyanto, "Maturity grading of oil palm fresh fruit bunches based on a machine learning approach," *2020 5th International Conference on Informatics and Computing, ICIC 2020*, Nov. 2020, doi: [10.1109/ICIC50835.2020.9288603](https://doi.org/10.1109/ICIC50835.2020.9288603).
- [5] A. Septiarini, A. Sunyoto, H. Hamdani, A. A. Kasim, F. Utamingrum, and H. R. Hatta, "Machine vision for the maturity classification of oil palm fresh fruit bunches based on color and texture features," *Sci Hortic*, vol. 286, p. 110245, Aug. 2021, doi: [10.1016/J.SCIENTA.2021.110245](https://doi.org/10.1016/J.SCIENTA.2021.110245).
- [6] C. Anam, M. Informatika, S. Tinggi Ilmu Komputer PGRI Banyuwangi, and J. Timur, "Mobile e-detection of Banyuwangi's citrus fruit maturity using k-nearest neighbor," *Jurnal Informatika*, vol. 14, no. 3, pp. 112–118, Sep. 2020, doi: [10.26555/JIFO.V14I3.A18183](https://doi.org/10.26555/JIFO.V14I3.A18183).
- [7] J. Gené-Mola *et al.*, "Fruit detection in an apple orchard using a mobile terrestrial laser scanner," *Biosyst Eng*, vol. 187, pp. 171–184, Nov. 2019, doi: [10.1016/J.BIOSYSTEMSENG.2019.08.017](https://doi.org/10.1016/J.BIOSYSTEMSENG.2019.08.017).
- [8] M. Fashi, L. Naderloo, and H. Javadikia, "The relationship between the appearance of pomegranate fruit and color and size of arils based on image processing," *Postharvest Biol Technol*, vol. 154, pp. 52–57, Aug. 2019, doi: [10.1016/J.POSTHARVBIO.2019.04.017](https://doi.org/10.1016/J.POSTHARVBIO.2019.04.017).
- [9] S. W. Sidehabi, A. Suyuti, I. S. Areni, and I. Nurtanio, "Classification on passion fruit's ripeness using K-means clustering and artificial neural network," *2018 International Conference on Information and Communications Technology, ICOIACT 2018*, vol. 2018-January, pp. 304–309, Apr. 2018, doi: [10.1109/ICOIACT.2018.8350728](https://doi.org/10.1109/ICOIACT.2018.8350728).
- [10] M. H. Malik, T. Zhang, H. Li, M. Zhang, S. Shabbir, and A. Saeed, "Mature Tomato Fruit Detection Algorithm Based on improved HSV and Watershed Algorithm," *IFAC-PapersOnLine*, vol. 51, no. 17, pp. 431–436, Jan. 2018, doi: [10.1016/J.IFACOL.2018.08.183](https://doi.org/10.1016/J.IFACOL.2018.08.183).
- [11] J. Lv, H. Ni, Q. Wang, B. Yang, and L. Xu, "A segmentation method of red apple image," *Sci Hortic*, vol. 256, p. 108615, Oct. 2019, doi: [10.1016/J.SCIENTA.2019.108615](https://doi.org/10.1016/J.SCIENTA.2019.108615).
- [12] W. Ji, Z. Qian, B. Xu, Y. Tao, D. Zhao, and S. Ding, "Apple tree branch segmentation from images with small gray-level difference for agricultural harvesting robot," *Optik (Stuttg)*, vol. 127, no. 23, pp. 11173–11182, Dec. 2016, doi: [10.1016/J.IJLEO.2016.09.044](https://doi.org/10.1016/J.IJLEO.2016.09.044).
- [13] R. Kestur, A. Meduri, and O. Narasipura, "MangoNet: A deep semantic segmentation architecture for a method to detect and count mangoes in an open orchard," *Eng Appl Artif Intell*, vol. 77, pp. 59–69, Jan. 2019, doi: [10.1016/J.ENGAPPAL.2018.09.011](https://doi.org/10.1016/J.ENGAPPAL.2018.09.011).

- [14] A. Durand-Petiteville, S. Vougioukas, and D. C. Slaughter, "Real-time segmentation of strawberry flesh and calyx from images of singulated strawberries during postharvest processing," *Comput Electron Agric*, vol. 142, pp. 298–313, Nov. 2017, doi: [10.1016/J.COMPAG.2017.09.011](https://doi.org/10.1016/J.COMPAG.2017.09.011).
- [15] A. Septiarini, H. Hamdani, H. R. Hatta, and K. Anwar, "Automatic image segmentation of oil palm fruits by applying the contour-based approach," *Sci Hortic*, vol. 261, p. 108939, Feb. 2020, doi: [10.1016/J.SCIENTA.2019.108939](https://doi.org/10.1016/J.SCIENTA.2019.108939).
- [16] R. Xiang, "Image segmentation for whole tomato plant recognition at night," *Comput Electron Agric*, vol. 154, pp. 434–442, Nov. 2018, doi: [10.1016/J.COMPAG.2018.09.034](https://doi.org/10.1016/J.COMPAG.2018.09.034).
- [17] U. O. Dorj, M. Lee, and S. seok Yun, "An yield estimation in citrus orchards via fruit detection and counting using image processing," *Comput Electron Agric*, vol. 140, pp. 103–112, Aug. 2017, doi: [10.1016/J.COMPAG.2017.05.019](https://doi.org/10.1016/J.COMPAG.2017.05.019).
- [18] Z. Wang, K. Wang, F. Yang, S. Pan, and Y. Han, "Image segmentation of overlapping leaves based on Chan–Vese model and Sobel operator," *Information Processing in Agriculture*, vol. 5, no. 1, pp. 1–10, Mar. 2018, doi: [10.1016/J.INPA.2017.09.005](https://doi.org/10.1016/J.INPA.2017.09.005).
- [19] H. Zhang, Q. Zhu, C. Fan, and D. Deng, "Image quality assessment based on Prewitt magnitude," *AEU - International Journal of Electronics and Communications*, vol. 67, no. 9, pp. 799–803, Sep. 2013, doi: [10.1016/J.AEUE.2013.04.001](https://doi.org/10.1016/J.AEUE.2013.04.001).
- [20] M. H. Hanafi, N. Fadillah, and A. Insan, "Optimasi Algoritma K-Nearest Neighbor untuk Klasifikasi Tingkat Kematangan Buah Alpukat Berdasarkan Warna," *IT Journal Research and Development*, vol. 4, no. 1, pp. 10–18, May 2019, doi: [10.25299/ITJRD.2019.VOL4\(1\).2477](https://doi.org/10.25299/ITJRD.2019.VOL4(1).2477).
- [21] C. Paramita, E. H. Rachmawanto, C. A. Sari, D. Rosal, and I. M. Setiadi, "Klasifikasi Jeruk Nipis Terhadap Tingkat Kematangan Buah Berdasarkan Fitur Warna Menggunakan K-Nearest Neighbor," *Jurnal Informatika: Jurnal Pengembangan IT*, vol. 4, no. 1, pp. 1–6, Jan. 2019, doi: [10.30591/JPIT.V4I1.1267](https://doi.org/10.30591/JPIT.V4I1.1267).
- [22] S. Aprilisa, J. Magister, I. Komputer, and S. J. Magister, "Klasifikasi Tingkat Kematangan Buah Tomat Berdasarkan Fitur Warna Menggunakan K-Nearest Neighbor," *Annual Research Seminar (ARS)*, vol. 5, no. 1, pp. 170–173, Feb. 2020, Accessed: Dec. 15, 2022. [Online]. Available: <https://seminar.ilkom.unsri.ac.id/index.php/ars/article/view/2134>
- [23] K. Tingkat, K. Buah, M. Menggunakan, and J. S. Tiruan..., "Klasifikasi Tingkat Kematangan Buah Markisa Menggunakan Jaringan Syaraf Tiruan Berbasis Pengolahan Citra Digital," *Journal of Embedded Systems, Security and Intelligent Systems*, vol. 1, no. 1, pp. 1–8, May 2020, doi: [10.26858/JESSI.V1I1.13505](https://doi.org/10.26858/JESSI.V1I1.13505).